

The simplest all-nitrogen ring: Photolytically filling the cyclic-N₃ well

Peter C. Samartzis

Department of Chemistry and Biochemistry, University of California Santa Barbara, Santa Barbara, California 93106

Jim Jr-Min Lin, Tao-Tsung Ching, and Chanchal Chaudhuri

Institute of Atomic and Molecular Sciences, Academia Sinica, P.O. Box 23-166, Taipei 106, Taiwan, Republic of China

Shih-Huang Lee

National Synchrotron Radiation Research Center, 101 Hsin-Ann Road, Hsinchu Science Park, Hsinchu 30076, Taiwan, Republic of China

Alec M. Wodtke^{a)}

Department of Chemistry and Biochemistry, University of California Santa Barbara, Santa Barbara, California 93106

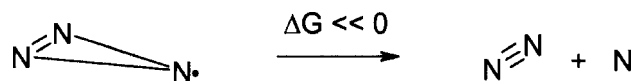
(Received 27 November 2006; accepted 20 December 2006; published online 23 January 2007)

We report evidence that *cyclic*-N₃ is exclusively produced in the 157-nm photolysis of ClN₃. Photoproduct translational energy measurements reveal a single-peaked distribution for an N₃-formation channel with maximum and minimum translational energies matching the theoretically predicted minimum and maximum binding energies of *cyclic*-N₃, respectively. The absence of linear-N₃ greatly simplifies the data analysis. The zero-Kelvin heat of formation of *cyclic*-N₃ is derived experimentally (142±3.5 kcal/mol) and is in excellent agreement with the best existing determinations from other studies. © 2007 American Institute of Physics.
[DOI: 10.1063/1.2433723]

The rich structural diversity of elemental carbon, which ranges from graphite to diamond to fullerenes and carbon nanotubes, teaches us that molecular ring formation is an essential requirement to allotropic diversity. Nitrogen, situated directly adjacent to carbon in the periodic table *appears*, by comparison, structurally barren. Since the discovery of N₂ in 1772,¹ only linear-N₃ (Ref. 2) (as well as its anion) have become common in chemistry. Developing new synthetic approaches for rings made from nitrogen atoms would provide a foothold into a broad, theoretically predicted³ area of “azidochemistry,” perhaps even leading to such remarkable molecules as the theoretically predicted N₆₀. The discovery of N₅AsF₆ in 1999, with N₅⁺ in a bent structure, became only the third all-nitrogen allotrope that could be prepared “in bulk” and stimulated renewed interest in the preparation of new homonuclear polynitrogen species.⁴ Shortly thereafter, N₄ was detected in minute quantities using neutralization re-ionization mass spectrometry but proved to be acyclic.⁵ Observation by mass spectrometry of the pentazolite anion, cyclic-N₅⁻ (Ref. 6) gave additional evidence for molecular rings made from nitrogen atoms; however, this species has thus far not been synthesized in significant quantities.⁷

The ability of nitrogen atoms to form closed, cyclic structures has been difficult to observe and means of producing them in significant quantities are unknown. Apart from cyclic-N₅⁻, detected in collision-induced-dissociation mass spectrometry,⁶ the possible existence of isolated cyclic nitro-

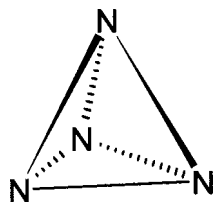
gen allotropes has remained largely a topic for theory and the question of how such molecules might be produced in the laboratory has remained unanswered. The difficulty in forming rings out of nitrogen atoms can be seen by considering the simplest cyclic all-nitrogen species and its dissociation



The third bond of the triple N–N bond has an approximate strength of 125 kcal/mol, whereas two N–N single bonds exhibit a combined binding energy of only about 80 kcal/mol. Furthermore, the molecule clearly exhibits substantial ring-strain energy and, by analogy with the cyclopropenyl radical,⁸ electronic antiaromatic⁹ destabilization.

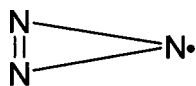
Partly due to the fact that this class of molecules is so unstable, they have been vigorously sought as materials capable of storing large amounts of energy in minimal mass or volume, so-called “high-energy-density materials.”¹⁰ In order to be experimentally useful, such species must be *metastable*, i.e., their spontaneous decomposition to N₂ must be inhibited by a substantial energetic barrier. The simplest all-nitrogen ring, *cyclic*-N₃, is quite interesting within this context, not only because it is theoretically predicted to be strongly bound, but because it is one of the most promising precursors for the long sought (see, for example, Ref. 11) N₄ allotrope, tetraazahedrane,¹² better known as tetrahedral-nitrogen, (*I*)

^{a)} Author to whom correspondence should be addressed. Electronic mail: wodtke@chem.ucsb.edu

**Molecule (1)**

Molecule (1) is illustrative of the chemical properties of this family of molecules. Formally in compliance with the octet-rule, it is a closed shell-species of singlet spin-multiplicity that would release more than 180 kcal/mol upon decomposition to two N_2 molecules.^{12,13} Theory calculates the barrier to decomposition to ground state N_2 to be greater than 60 kcal/mol, strongly suggesting that this species is isolable.¹³

Theoretical calculations suggest *cyclic-N₃* may undergo barrierless exoergic recombination with $N(^2D)$ -atoms to form tetraazahedrane.¹¹ Thus, simultaneous production of *cyclic-N₃* in the presence of $N(^2D)$ would appear to be a promising path to **molecule (1)**. High level *ab initio* calculations for *cyclic-N₃*, (**molecule (2)**), predict a C_{2v} structure of 2B_1 symmetry with two long (1.455 Å) and one short (1.218 Å) bonds, which may “pseudorotate” about a D_{3h} conical intersection.^{11,14,15}

**Molecule (2)**

Isomerization of *cyclic-N₃* to the well-known linear isomer (the azide radical) is exoergic by ~ 30 kcal/mol and spin-allowed but linearization must pass over a substantial 32 kcal/mol barrier with respect to the cyclic minimum. Likewise, theory predicts that dissociation to ground state $N(^4S_{3/2})$ and N_2 is exoergic by 31 kcal/mol, but is of course spin-forbidden. The lowest-energy spin-allowed dissociation channel forms $N(^2D)+N_2$ and is endoergic by 26 kcal/mol but, again, must pass over a dissociation barrier that is calculated to lie 33 kcal/mol above the *cyclic-N₃* minimum. Combining the most accurate experimental heat of formation for linear- N_3 (Ref. 16) with the theoretical calculation of the ring-closing energy above provides the most accurate prediction of the zero-Kelvin heat of the formation of *cyclic-N₃*, $\Delta H_F(\text{cyc-N}_3)=144\pm 2$ kcal/mol.

Tantalizing evidence that *cyclic-N₃* and *linear-N₃* can be produced simultaneously by UV photolysis is accumulating in the literature. In a velocity map imaging (VMI) study of ClN_3 photolysis at 235 nm, Hansen and Wodtke¹⁷ detected bimodal translational energy distribution for the Cl photofragments, whose energetic splitting matched the N_3 cyclization energy. The N_3 formed with the “slow-Cl” corresponds to a *highly internally excited form* of N_3 (*HEF-N₃*). This experiment could be used to extract an estimate of ΔH_F (*HEF-N₃*), which was consistent with that of *cyclic-N₃*, but the simultaneous production of linear- N_3 complicated the analysis, leaving open the possibility that dynamical mecha-

nisms might be capable of producing linear- N_3 with a bimodal internal energy distribution. Photofragmentation translational spectroscopy (PTS) experiments of ClN_3 photolysis at 248 nm, using electron impact¹⁸ to ionize the photofragments again showed production of two forms of N_3 with an energetic splitting close to the N_3 cyclization energy. More importantly, this work provided direct detection of *HEF-N₃*. Later, synchrotron radiation was used to measure the ionization threshold of *HEF-N₃* (10.67 ± 0.2 eV),¹⁹ which was in reasonable agreement with theoretical predictions for *cyclic-N₃*.²⁰ In addition, H-atom Rydberg tagging experiments on the wavelength dependent photolysis of HN_3 showed production of low translational energy H-atoms only at photolysis energies above a theoretically predicted ring closing transition state on the S_1 HN_3 hypersurface.²¹ Despite this body of evidence, definitive evidence proving the photolytic production of *cyclic-N₃* is still lacking.

In this paper we present evidence obtained by PTS experiments on 157 nm ClN_3 photolysis showing that N_3 is produced within a range of internal energies matching the energy extent of the theoretically predicted *cyclic-N₃* well. Short of direct spectroscopic characterization, we consider this to be the best possible direct evidence for the photolytic production of *cyclic-N₃*. This provides an accurate experimental derivation of the upper limit to the heat of formation of the *cyclic-N₃* in the absence of any contaminating linear- N_3 impurity, greatly simplifying the data analysis leading to an experimental heat of formation for *cyclic-N₃*, as well as the height of the *cyclic-N₃* dissociation barrier. Both of these experimental quantities are in excellent agreement with theoretical predictions.

A description of the apparatus used in this work has been previously published¹⁹ and only a brief description is given here. We employ vacuum-ultraviolet synchrotron-radiation to ionize and detect the collision-free photofragments produced by 157-nm laser photodissociation of a molecular beam of ClN_3 , measuring the deflection-angle-resolved photofragment neutral time-of-flight (TOF) distributions. The work was carried out at beamline 21A of the National Synchrotron Radiation Research Center in Hsinchu, Taiwan. More specifically, we employ ionizing photon-energies ($h\nu$) between 14 and 16 eV. The photon-energy spread ($\delta h\nu/h\nu$) of the synchrotron radiation is $\sim 3\%$ full width at half maximum (FWHM). Higher order harmonics produced by the beamline undulator were filtered by appropriate noble gases in a separate harmonic separator chamber.²² In this way we are able to ionize all of the ClN_3 photolysis products and detect the parent ions in the absence of dissociative ionization, greatly simplifying the data analysis. ClN_3 is prepared by reaction of a 10% Cl_2 mix in He with moist NaN_3 suspended in cotton wool. The mixture (now containing ClN_3) passes through a drying agent (Drierite) to remove excess water and forms a supersonically cooled molecular beam expanding into the source chamber of the apparatus. Typically, the molecular beam velocity is 1100 m/s with a speed ratio of 10. The molecular beam is crossed at right angles by the focused output (3 mm in the direction of the neutral TOF axis $\times 9$ mm perpendicular to the TOF axis) of an excimer laser operating at 157 nm which dissociates ClN_3 . The photofrag-

ments are allowed to fly 100.5 mm through two separate differentially pumped chambers before being ionized by a beam of synchrotron radiation (1.0×1.0 mm spot size) in a cryogenically cooled ultrahigh vacuum chamber. The photoions produced in this way are mass selected by a quadrupole mass filter and the mass-to-charge (m/z) ratio of choice was detected by a Daly-style ion detector and counted by a multichannel scaler. We use the rotateable molecular beam source to measure the TOF spectra of all photofragments ($m/z=42, 35, 28, 49$ and 14) produced in the photolysis of ClN_3 at 157 nm at three laboratory angles $\Theta=20^\circ, 40^\circ$, and 60° , between the molecular beam and the TOF detection axis. Each TOF spectrum was averaged for 10^4 – 10^5 laser shots as needed to provide adequate signal-to-noise.

The observed TOF data are quantitatively explained by reactions (R1) and (R2)



In addition, reaction (R3) is a very minor but observable contributor to the photochemistry at 157 nm



We used the PHOTRAN as well as ANALMAX²³ forward-convolution programs to fit laboratory-frame primary and secondary dissociation TOF data with optimized center-of-mass (COM) frame relative translational-energy release distributions, $P(E_T)$. PHOTRAN simulates the TOF spectrum based on a COM total translational energy distribution, $P(E_T)$, which is iteratively adjusted until a satisfactory fit to the data is obtained. Beam velocity, laboratory angle Θ , dissociation and ionization interaction-volume sizes, finite angular acceptance angle of the detector, laser power and polarization are additional program parameters used to simulate the experiment. The major sources of error in the determination of the translational energy is uncertainty in the molecular beam velocity and in the ion flight time, that is the time required for the photoion produced by the synchrotron radiation to transit the quadrupole mass filter and reach the Daly-style ion detector. Horizontal error bars for $P(E)$ are obtained by fitting the TOF data using a range of average beam velocities and ion flight times, varying these within their known range of uncertainties. This range is shown as horizontal error bars in Fig. 2. The derived $P(E_T)$ s for the three reactions provide accurate energy release information and limiting energetics determined by the heats of formation and heights of dissociation barriers of the photoreactant and products.

In this communication, we focus on the dominant channel, reactions (R1) and (R2). The N₃ TOF spectrum recorded at a laboratory angle $\Theta=40^\circ$ is shown in Fig. 1(a) and compared to the Cl TOF spectrum [Fig. 1(b)]. The COM translational energy distribution leading to stable N₃, $P_{\text{N}_3}(E_T)$, shown in Fig. 2, was optimized to accurately reproduce N₃ TOF data [e.g., the solid line in Fig. 1(a)] at all three recoil angles, $\Theta=20^\circ, 40^\circ$, and 60° . $P_{\text{N}_3}(E_T)$ was then used to simulate the Cl-TOF spectrum [solid line in Fig. 1(b)], which is constrained by linear momentum conservation. The de-

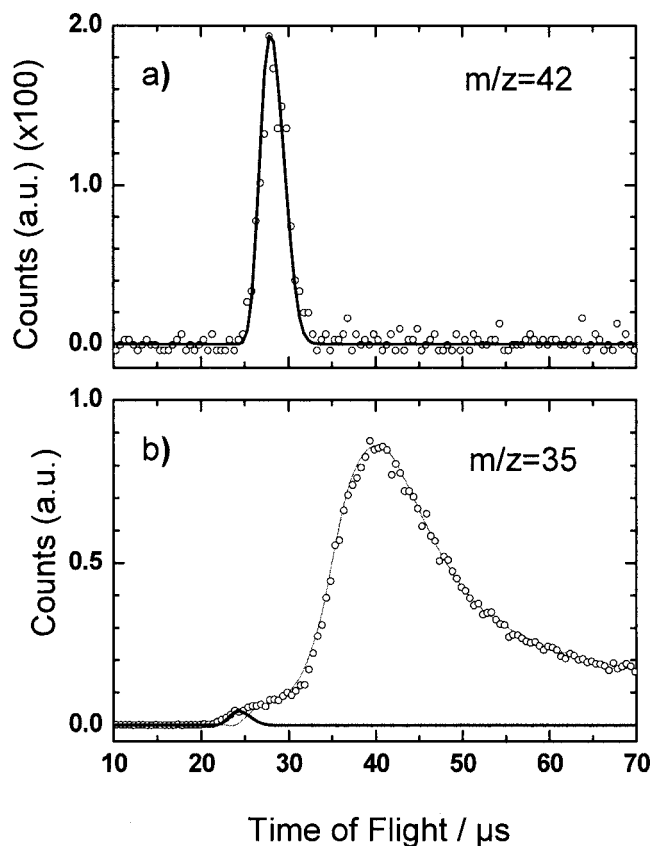


FIG. 1. Experimental TOF spectra of (a) $m/z=42$ (N_3^+) and (b) $m/z=35$ (Cl^+) at laboratory deflection angle, $\Theta=40^\circ$, and 15.9 eV ionization photon energy. The experimental data are presented as open circles. Thick solid lines indicate the contributions to the TOF data from reaction (R1), that is only those translational energies where stable N₃ is observed. The derived COM translational energy distribution corresponding to this component can be seen in Fig. 2. The thin gray line in (b) represents the portion of reaction (R1) forming N₃ with sufficient energy to lead to dissociation, reaction (R2), where only the Cl-product is detected. This fit was derived from another translational energy distribution, referred to as $P_{\text{slow}}(E_T)$ (not shown).

rived $P_{\text{N}_3}(E_T)$ shows that N₃ is only observed when the COM translational energy release lies within certain limits: $111 \pm 3.5 > E_T > 72 \pm 3.5$ kcal/mol. Closer inspection of Fig. 1 reveals that Cl atoms appearing at arrival times greater than about $25 \mu\text{s}$ (corresponding to COM translational energies less than 72 ± 3.5 kcal/mol), do not appear with an N₃ counterpart. One immediately realizes that these “slow Cl atoms” are formed with internally excited N₃ that has dissociated [by reaction (R2)] before reaching the detector.

A detailed description of the secondary dissociation analysis for reaction (R2) is beyond the scope of this paper; however, we note that all of the data is explained quantitatively by reactions (R1)–(R3). We include a brief description and some examples of secondary analysis in the on-line supplementary material.²⁸ An extensive presentation of the secondary analysis will appear in a future paper.

The derived energy distribution, $P_{\text{N}_3}(E_T)$, provides compelling evidence for cyclic-N₃ formation. However, this only became clear after a recent comprehensive experimental and theoretical study of the dissociative photoionization of ClN_3 led to a significant downward revision of the $D_0(\text{Cl}-\text{N}_3)$

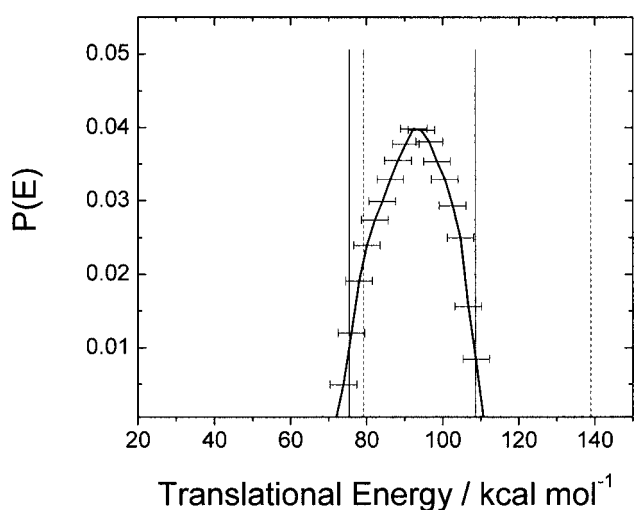


FIG. 2. Total center-of-mass frame translational energy release distribution used to simulate the $m/z=42$ TOF data. Solid drop-down lines show the predicted minimum and maximum translational energies for the Cl + *cyclic*-N₃ and dashed drop-down lines the minimum and maximum translational energies for the Cl + *linear*-N₃ following photolysis of ClN₃ at 157 nm. The error bars reflect the uncertainty in ion flight time, molecular beam velocity and other experimental parameters. The excellent agreement with the predictions for *cyclic*-N₃ provides proof of exclusive production of cyclic N₃ under our experimental conditions.

$=43 \pm 1$ kcal/mol²⁴ (from 49.6 kcal/mol¹⁷) and an upward revision of the $\Delta H_f(\text{ClN}_3)=99 \pm 1$ kcal/mol²⁴ (from 93 kcal/mol¹⁷). Using the 157.6 nm photon energy ($h\nu_{\text{photolysis}}=181.4$ kcal/mol) and $D_0(\text{Cl-N}_3)$ dissociating to *linear*-N₃) $=43 \pm 1$ kcal/mol,²⁴ we calculate the energy available to the photofragments, $E_{\text{ava}}=138$ kcal mol⁻¹. This is the maximum translational energy expected if Cl and *linear*-N₃ were formed with no internal energy and is shown as a dashed line in Fig. 2. The dissociation threshold for *linear*-N₃ has been calculated with high-level electronic structure theory to be 59.6 ± 2 kcal/mol.¹⁵ Thus, if *linear*-N₃ were formed, we would expect N₃ dissociation at translational energies less than 78.4 kcal/mol. This is also shown as a dashed line in Fig. 2.

We may repeat this analysis assuming exclusive production of *cyclic*-N₃. Here the available energy ($E_{\text{ava}}=108$ kcal/mol, shown in Fig. 2 as a solid vertical line) is reduced in comparison to the previous analysis by the cyclization energy of N₃, 30.3 kcal/mol.¹⁵ The calculated dissociation energy of *cyclic*-N₃ (63.4 kcal/mol above the *linear*-N₃ energy) limits the translational energy where N₃ TOF signal can appear to values corresponding to greater than 74.6 kcal/mol, also shown as a vertical solid line in Fig. 2. Thus, this analysis predicts *cyclic*-N₃ fragments only within the range of translational energies: $108 \pm 2.5 > E_T > 75 \pm 2.5$ kcal/mol, in excellent agreement with observation: $111 \pm 3.5 > E_T > 72 \pm 3.5$ kcal/mol (see Fig. 2). This straightforward energy balancing analysis leads us to conclude that dissociation of ClN₃ at 157 nm exclusively produces *cyclic*-N₃, with internal energies distributed across all possible values contained within the bonding well.

This can be seen perhaps more clearly in Fig. 3, where we show all energetically accessible states of N₃ compared to the observed range of N₃ energies (demarcated as five-

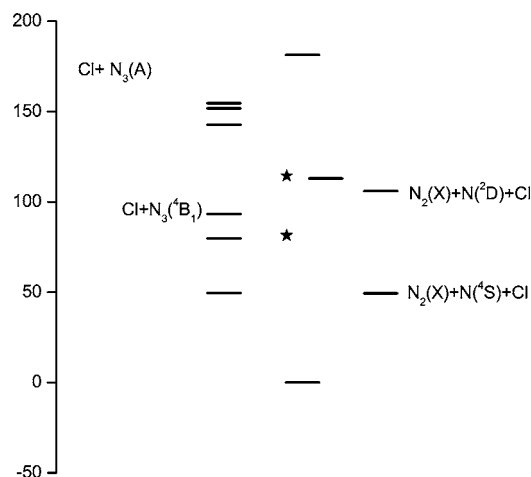


FIG. 3. Energetics for various states of N₃ that might be produced in the 157 nm photolysis of ClN₃ at 157.6 nm. The energy of ClN₃ is taken as zero. Stars designate the minimum and maximum internal energies of N₃ detected in this experiment.

pointed stars). Although many states of N₃ are energetically accessible, including $A^2\Sigma$, $B^2\Pi$, $\alpha^4\Pi$, and another quartet excited state of N₃, $4B_1$, none of these processes can explain our observations. By comparison, the observed maximum and minimum translational energy release values (marked as five-pointed stars in Fig. 3) coincide well with the *cyclic*-N₃ minimum and dissociation barrier, respectively, and provide a straightforward explanation of the observations.

This work can also be used to obtain a purely experimental determination of $\Delta H_f^0(\text{cyc-N}_3)$ under conditions where *linear*-N₃ formation does not obscure the maximum translational energy release

$$\begin{aligned} \Delta H_f^0(\text{cyc-N}_3) &= \Delta H_f^0(\text{ClN}_3) + h\nu - \Delta H_f^0(\text{Cl}) - E_T^{\text{MAX}} \\ &= (99 + 181.4 - 28.5 - 111) \text{ kcal/mol} \\ &= 140.9 \pm 3.5 \text{ kcal/mol.} \end{aligned} \quad (1)$$

Previously, the best value for the $\Delta H_f^0(\text{cyc-N}_3)$ came from published work employing the highly accurate $\Delta H_f^0(\text{lin-N}_3)=113.6$ kcal/mol^{16,25} and high level calculations of the cyclization energy (30.3 kcal/mol) of *linear* N₃,¹⁵ leading to $\Delta H_f^0(\text{cyc-N}_3)=144 \pm 2$ kcal/mol.¹⁵ Another recent paper on ClN₃ photolysis at 193 nm, reported a maximum translational energy release, $E_T^{\text{MAX}}=77 \pm 3$ kcal/mol and commented that the products were produced with an unexpectedly large amount of internal energy.²⁶ If we postulate that the 193-nm photolysis of ClN₃ also produces *cyclic*-N₃ exclusively, we can use Eq. (1) to independently derive the zero-Kelvin heat of formation of *cyclic* N₃: $\Delta H_f^0(\text{cyc-N}_3)=(99+147.9-28.5-77)$ kcal/mol $=141.5 \pm 3$ kcal/mol, in excellent agreement with the results presented above. Furthermore, values for $\Delta H_f^0(\text{cyc-N}_3)$ may be derived from earlier work where the photolysis wavelengths of 235 and 248 nm were employed. Here *linear* N₃ was clearly identified at high translational energy release, obscuring the maximum translational energy release of the high energy form. Those results, which are less accurate due to the production of

two forms of N₃ are nevertheless, quantitatively consistent with the picture presented above.

The fact that these four experiments at different photolysis wavelengths, carried out under conditions where the available energy to the cyclic-N₃ product formation channel varied between 43 and 110 kcal/mol, yet produce the same energetic result is strong evidence that all of these experiments observe the same chemical species with a defined heat of formation, as opposed to some alternative dynamical explanation. This implies that the previously reported *HEF*-N₃ is indeed *cyclic*-N₃.

Perhaps of greatest significance, these results suggest approaches to the production of *cyclic*-N₃ in the condensed phase for the purpose of exploring its chemical reactivity, spectroscopy and the geometric phase effect²⁷ in *cyclic*-N₃. Commercially available KrF (248 nm) lasers are now capable of producing mmols of photons per second. Thus, there is no fundamental reason why production of *cyclic*-N₃ to initiate new chemistry could not be scaled to gram quantities, either in the gas-phase or in inert solvents such as supercritical CO₂, liquid argon or nitrogen. Furthermore, UV photolysis of ClN₃ in a cryogenic rare gas solvent could be carried out under conditions where *cyclic*-N₃ and N(²D) are formed together, possibly leading to conditions where tetraazaheptane, *molecule (I)*, might be produced in significant quantity.¹¹

This work was in part supported by a grant from the Air Force Office of Scientific Research (Grant No. FA9550-04-1-0057). We thank Institute of Atomic and Molecular Sciences, Academia Sinica, Taipei, Taiwan for financial support and the National Synchrotron Radiation Research Center personnel for their help in conducting those experiments.

¹D. Rutherford, M.D. thesis, University of Edinburgh, 1772.

²T. Curtius, *Berichte d. D. chem. Gesellschaft* **Jahrgang XXIII** **2**, 3023 (1890); B. A. Thrush, *Proc. R. Soc. London, Ser. A* **235**, 143 (1956).

³R. J. Bartlett, *Chem. Ind.* **4**, 140 (2000).

⁴K. O. Christe, W. W. Wilson, J. A. Sheehy, and J. A. Boatz, *Angew. Chem., Int. Ed. Engl.* **38**, 2004 (1999).

⁵F. Cacace, G. de Petris, and A. Troiani, *Science* **295**, 480 (2002).

⁶A. Vij, J. G. Pavlovich, W. W. Wilson, V. Vij, and K. O. Christe, *Angew. Chem., Int. Ed. Engl.* **41**, 3051 (2002).

⁷T. Schroer, R. Haiges, S. Schneider, and K. O. Christe, *Chem. Commun. (Cambridge)* **12**, 1607 (2005).

⁸K. Schreiner, W. Ahrens, and A. Berndt, *Angew. Chem., Int. Ed. Engl.* **14**, 550 (1975); A. D. Allen and T. T. Tidwell, *Chem. Rev. (Washington, D.C.)* **101**, 1333 (2001).

⁹R. Breslow, J. Brown, and J. J. Gajewski, *J. Am. Chem. Soc.* **89**, 4383 (1967).

¹⁰A. Friedmann, A. M. Soliva, S. A. Nizkorodov, E. J. Bieske, and J. P. Maier, *J. Phys. Chem.* **98**, 8896 (1994).

¹¹M. Bittererova, H. Ostmark, and T. Brinck, *J. Chem. Phys.* **116**, 9740 (2002).

¹²T. J. Lee and J. M. L. Martin, *Chem. Phys. Lett.* **357**, 319 (2002).

¹³K. M. Dunn and K. Morokuma, *J. Chem. Phys.* **102**, 4904 (1995).

¹⁴D. Babikov, P. Zhang, and K. Morokuma, *J. Chem. Phys.* **121**, 6743 (2004).

¹⁵P. Zhang, K. Morokuma, and A. M. Wodtke, *J. Chem. Phys.* **122**, 014106 (2005).

¹⁶R. E. Continetti, D. R. Cyr, D. L. Osborn, D. J. Leahy, and D. M. Neumark, *J. Chem. Phys.* **99**, 2616 (1993).

¹⁷N. Hansen and A. M. Wodtke, *J. Phys. Chem. A* **107**, 10608 (2003).

¹⁸N. Hansen, A. M. Wodtke, S. J. Goncher, J. C. Robinson, N. E. Sveum, and D. M. Neumark, *J. Chem. Phys.* **123**, 104305 (2005).

¹⁹P. C. Samartzis, J. J. M. Lin, T. T. Ching, C. Chaudhuri, Y. T. Lee, S. H. Lee, and A. M. Wodtke, *J. Chem. Phys.* **123**, 051101 (2005).

²⁰R. Tarroni and P. Tosi, *Chem. Phys. Lett.* **389**, 274 (2004); D. Babikov, V. A. Mozhayskiy, and A. I. Krylov, *J. Chem. Phys.* **125**, 084306 (2006); V. A. Mozhayskiy, D. Babikov, and A. I. Krylov, *ibid.* **124**, 224309 (2006).

²¹J. Zhang, Y. Chen, K. Yuan, S. A. Harich, X. Wang, X. Yang, P. Zhang, Z. Wang, K. Morokuma, and A. M. Wodtke, *Phys. Chem. Chem. Phys.* **8**, 1690 (2006).

²²A. G. Suits, P. Heimann, X. M. Yang, M. Evans, C. W. Hsu, K. T. Lu, Y. T. Lee, and A. H. Kung, *Rev. Sci. Instrum.* **66**, 4841 (1995).

²³A. M. Wodtke, Ph.D. thesis, University of California, Berkeley, 1986.

²⁴A. Quinto, Y. Y. Lee, T. P. Huang, W. C. Pan, J. M. Lin, P. Bobadova-Parvanova, K. Morokuma, P. Samartzis, and A. M. Wodtke, *Int. J. Mass. Spectrom.* (submitted).

²⁵R. E. Continetti, D. R. Cyr, R. B. Metz, and D. M. Neumark, *Chem. Phys. Lett.* **182**, 406 (1991).

²⁶S. J. Goncher, N. E. Sveum, D. T. Moore, N. D. Bartlett, and D. M. Neumark, *J. Chem. Phys.* **125**, 224304 (2006).

²⁷D. Babikov, B. K. Kendrick, P. Zhang, and K. Morokuma, *J. Chem. Phys.* **122**, 044315 (2005).

²⁸See EPAPS Document No. E-JCPSA6-126-032704 for a brief description of the secondary analysis. This document can be reached via a direct link in the online article's HTML reference section or via the EPAPS homepage (<http://www.aip.org/pubservs/epaps.html>).